

**FUNCTIONALLY GRADED NiTi SHAPE  
MEMORY ALLOYS BY AGEING AND PARTIAL  
ANNEALING**

**MUHAMMAD NAQIB BIN NASHRUDIN**

**UNIVERSITI SAINS MALAYSIA**

**2018**

**FUNCTIONALLY GRADED NiTi SHAPE MEMORY ALLOYS BY AGEING  
AND PARTIAL ANNEALING**

**by**

**MUHAMMAD NAQIB BIN NASHRUDIN**

**Thesis submitted in fulfilment of the  
requirements for the Degree of  
Master of Science**

**July 2018**

## ACKNOWLEDGEMENT

Alhamdulillah, all praise to Allah SWT, who has answered all my prayers and eased the completion of this research work.

I am in-debted to my supervisor, Assoc. Prof. Ir. Dr. Abdus Samad bin Mahmud for his insightful mentoring throughout the project. With his guidance, I was able to conduct the research systematically and be able to complete it in a timely manner. My appreciation also goes to the research members in the Nano Fabrication and Materials Lab, School of Mechanical Engineering, USM, who have provided support in terms of technical knowledge related to the project. Not forgetting, the technical and support staff at the School of Mechanical Engineering, USM, who have assisted in sample preparations, analysis and experimentations. Their contributions are greatly appreciated.

Special thanks go to my family and friends, especially my parents, Nashrudin bin A. Rahman and Norashikin binti Mohd. Nordin for their encouragements and confidence in me to complete the study successfully.

Finally, I would like to acknowledge and express my gratitude for the financial support provided by the Ministry of Higher Education (MOHE), Malaysia under the MyBrain programme (MyMaster) and the Graduate Research Assistance (GRA) scheme, USM, for the tuition and subsistence allowances throughout the duration of the study.

Muhammad Naqib bin Nashrudin

July 2018

## TABLE OF CONTENTS

	<b>Page</b>
<b>ACKNOWLEDGEMENT</b>	ii
<b>TABLE OF CONTENTS</b>	iii
<b>LIST OF TABLES</b>	vii
<b>LIST OF FIGURES</b>	viii
<b>LIST OF ABBREVIATIONS</b>	xiii
<b>LIST OF SYMBOLS</b>	xiv
<b>ABSTRAK</b>	xv
<b>ABSTRACT</b>	xvii
<b>CHAPTER ONE : INTRODUCTION</b>	<b>Page</b>
1.1 Research Background	1
1.2 Problem Statement	5
1.3 Objectives	8
1.4 Scope of work	8
<b>CHAPTER TWO : LITERATURE REVIEW</b>	
2.1 The mechanism of shape memory behavior	9
2.1.1 Thermoelastic martensitic transformation	9
2.1.2 Self-accommodation of lattice distortion	10

2.1.3	Thermomechanical behavior	11
2.2	NiTi shape memory alloy	13
2.2.1	Phase diagram	14
2.2.2	Crystal structure of NiTi shape memory alloy	15
2.3	Shape memory behavior of NiTi	16
2.3.1	Thermal martensite phase transformation	16
2.3.2	Stress-induced martensite phase transformation behavior	19
2.4	Thermomechanical treatment	23
2.4.1	Cold working and annealing treatment	24
2.4.2	Effect of anneal on thermal transformation behavior	25
2.4.3	Effect of partial anneal on mechanical behavior	27
2.4.4	Ageing treatment	30
2.4.5	Process of precipitation	31
2.4.6	Effect of ageing on thermal transformation behavior	35
2.4.7	Effect of ageing on mechanical behavior	37
2.5	Gradient behavior	40
2.5.1	Gradient annealed behavior	41
2.5.2	Gradient aged behavior	42
2.5.3	Geometrically graded NiTi	44
2.6	Laser heat treatment on NiTi alloy	45
2.6.1	CO <sub>2</sub> laser design	46
2.6.2	Local annealing by laser beam	46

2.6.3	Functionally graded NiTi thin plate by laser annealing	47
2.7	Summary	48

### **CHAPTER THREE : METHODOLOGY**

3.1	Procedure overview	50
3.2	Experimental procedure	51
3.2.1	Solution treatment in vacuum condition and cold work process	52
3.2.2	Isothermal heat treatment	54
3.2.3	Martensitic transformation temperature analysis	55
3.2.4	Tensile deformation behavior analysis	57
3.3	Localized heat treatment	59
3.3.1	CO <sub>2</sub> laser setup	59
3.3.2	Localization of gradient and stepped heat treatment	61

### **CHAPTER FOUR : RESULTS AND DISCUSSION**

4.1	Effect of heat treatment on thermal transformation behavior	64
4.2	Effect of heat treatment temperatures on deformation behavior	75
4.3	Gradient shape memory deformation behavior	79
4.4	Thermal transformation behavior verification	86

<b>CHAPTER FIVE : CONCLUSION AND FUTURE WORKS</b>	90
5.1 Suggestions for future developments	92
<b>REFERENCES</b>	93
<b>LIST OF PUBLICATIONS</b>	

## LIST OF TABLES

		<b>Page</b>
Table 4.1	The transformation temperatures of isothermal heat treatment of NiTi specimens.	72

## LIST OF FIGURES

		<b>Page</b>
Figure 1.1	A graphic illustration of (a) shape memory effect and (b) pseudoelasticity exhibited by shape memory alloys.	2
Figure 1.2	Stress-strain curve showing the pseudoelastic deformation behavior.	3
Figure 1.3	Deformation behavior of gradient-annealed Ti-50.5at%Ni alloy.	6
Figure 1.4	Stress-strain curve of gradient ageing Ti-50.8at%Ni.	7
Figure 2.1	Illustration diagram of diffusionless and diffusive solid phase transformation.	10
Figure 2.2	Illustration diagram of self-accomodation of martensite.	11
Figure 2.3	SMA phases and crystal structures.	13
Figure 2.4	Phase diagram of NiTi alloys.	14
Figure 2.5	Crystal structures of (a) austenite, (b) martensite and (c) R-phase.	15
Figure 2.6	Thermal transformation temperature.	17
Figure 2.7	Graph of $M_s$ temperature against Ni content (at%).	18
Figure 2.8	Multi-stage transformation temperature.	19
Figure 2.9	Tensile deformation behavior of pseudoelastic NiTi.	20
Figure 2.10	Tensile deformation behaviors of NiTi alloy at different temperatures.	21
Figure 2.11	Stress-strain curves showing the deformation behavior of NiTi alloy at different testing temperatures.	22
Figure 2.12	The effect of testing temperature on critical stresses for the stress-induced martensitic transformations.	23
Figure 2.13	Thermal transformation behavior of partial annealed of cold-worked Ti-50.5at%Ni at various temperatures for 1 hour.	25

Figure 2.14	Effect of annealing temperature towards transformation temperature of near-equiatomic NiTi.	27
Figure 2.15	Effect of partial anneal treatment on tensile deformation for cold-worked Ti-49.8at%Ni.	28
Figure 2.16	Cold-worked NiTi annealed at 350°C to 650°C for 10 minutes.	29
Figure 2.17	Effect of annealing temperature of both forward and reverse deformation behavior for (a) critical stresses and (b) plateau strains.	30
Figure 2.18	Phase diagram of Ni-rich NiTi alloy.	31
Figure 2.19	Time-temperature-transformation diagram of Ti-52at%Ni alloy.	32
Figure 2.20	TEM micrograph showing the precipitates nucleate close to the grain boundaries after ageing NiTi of Ti-50.7at%Ni at 500°C (773K) for (a) 1 hour and (b) 10 hours.	33
Figure 2.21	TEM images showing the growing of Ti <sub>3</sub> Ni <sub>4</sub> precipitates microstructure after ageing solutionized Ti-50.9at%Ni for 1.5 hours at (a) 623 K, (b) 673 K, (c) 723 K, (d) 773 K and (e) 823 K.	34
Figure 2.22	Effect of ageing on transformation behavior of Ti-50.9at%Ni.	36
Figure 2.23	Effect of ageing temperature and duration on A <sub>r</sub> temperature of Ti-50.7at%Ni alloy.	37
Figure 2.24	Stress-strain curve of Ti-50.9at%Ni deformed at testing temperature of 310 K.	38
Figure 2.25	Effect of ageing treatment on forward and reverse plateau of Ti-50.7at%Ni stent wire.	39
Figure 2.26	Effect of ageing temperature on the critical stress and the yield strength of the stress-induced martensite of Ti-50.9at%Ni alloy.	40
Figure 2.27	Stress-strain curves of isothermally annealed of Ti-50.2at%Ni.	41
Figure 2.28	Stress-strain curve of gradient-annealed Ti-50.2at%Ni alloy.	42

Figure 2.29	Selected isothermal ageing temperature range for functionally graded treatment.	43
Figure 2.30	Stress-strain curve of gradient ageing of Ti-50.8at%Ni alloy.	44
Figure 2.31	Stress-strain curves of geometrically graded NiTi (a) linear strips, (b) concave strips and (c) convex strips.	45
Figure 2.32	The schematic setup of the CO <sub>2</sub> laser.	46
Figure 2.33	Shape memory alloy gripper that had been locally annealed (the black area).	47
Figure 2.34	SEM micrograph showing the effect of surface laser anneal within the thickness of the plate.	48
Figure 3.1	Flow chart showing the experimental design and procedures.	51
Figure 3.2	The setup of vacuum process.	53
Figure 3.3	Schematic diagram of vacuum process.	53
Figure 3.4	NiTi wires sealed in quartz tube.	54
Figure 3.5	Cold working process.	54
Figure 3.6	TA Q20 Differential Scanning Calorimeter (DSC).	55
Figure 3.7	Schematic illustration showing the determination of the thermal phase transformation temperatures from the DSC curve.	56
Figure 3.8	Instron 3367 universal testing machine (UTM).	57
Figure 3.9	Illustration of measurements of transformation stress and transformation strain from the stress-strain curve.	58
Figure 3.10	CO <sub>2</sub> laser setup.	59
Figure 3.11	Schematic diagram of CO <sub>2</sub> laser setup.	60
Figure 3.12	The position of NiTi wire on jig.	61
Figure 3.13	Schematic diagram of jig.	61

Figure 3.14	The position of thermocouples.	62
Figure 3.15	Real time plot of temperature recorded by six thermocouples (TC) for 400°C in 10 minutes of gradient heat treatment.	63
Figure 3.16	Sectioning of DSC specimen from the gauge length of gradient heat treatment specimen.	63
Figure 4.1	Thermal transformation behavior of cold worked Ti-50.9at%Ni alloy after heat treated at 500°C at different duration.	66
Figure 4.2	Thermal transformation behavior of Ti-50.9at%Ni alloy after heat treated at different temperature for 10 minutes.	68
Figure 4.3	Thermal transformation behavior of Ti-50.9at%Ni alloy after heat treated at different temperature for 20 minutes.	69
Figure 4.4	Thermal transformation behavior of Ti-50.9at%Ni alloy after heat treated at different temperature for 30 minutes.	70
Figure 4.5	Thermal transformation behavior of Ti-50.9at%Ni alloy after heat treated at different temperature for 60 minutes.	71
Figure 4.6	Effect of heat treatment temperature for 20 minutes on (a) transformation peak temperatures and (b) transformation latent heats.	74
Figure 4.7	Tensile deformation behavior of cold worked Ti-50.9at%Ni after heat treated at different temperatures for (a) 10 min, (b) 20 min, (c) 30 min and (d) 60 min.	76
Figure 4.8	Effect of heat treatment on plateau stress level.	78
Figure 4.9	Effect of heat treatment on residual strain.	79
Figure 4.10	The selection of heat treatment temperature and duration for gradient deformation; (a) forward transformation and (b) reverse transformation.	80
Figure 4.11	Effect of heat treatment temperature on stress-induced martensite phase transformation and residual strain for (a) range 1 and (b) range 2.	82
Figure 4.12	The position of local heat treatment along a wire.	82
Figure 4.13	Step gradient deformation behavior of cold-worked Ti-50.9at%Ni wire for (a) range 1 and (b) range 2.	85

Figure 4.14	Thermal transformation behavior of local heat treatment for range 1 gradient specimen.	87
Figure 4.15	Thermal transformation behavior of local heat treatment for range 2 gradient specimen.	89

## LIST OF ABBREVIATIONS

SMA	Shape Memory Alloy
DSC	Differential Scanning Calorimeter
UTM	Universal Testing Machine
NiTi	Nickel Titanium
Ti <sub>3</sub> Ni <sub>4</sub>	Nickel Titanium precipitate
TiNi <sub>3</sub>	Nickel Titanium precipitate
Ti <sub>2</sub> Ni <sub>3</sub>	Nickel Titanium precipitate
Au-Cd	Gold-Cadmium
Cu-Zn	Copper-Zinc
Cu-Zn-Al	Copper-Zinc-Aluminum
Fe-Mn-Si	Iron-Manganese-Silicon
Cu-Al-Ni	Copper-Aluminum-Nickel
CsCl	Caesium Chloride

## LIST OF SYMBOLS

%	Percentage
T	Temperature
TC	Thermocouple
CO <sub>2</sub>	Carbon dioxide
$\varepsilon$	Strain
M <sub>s</sub>	Martensite start
M <sub>f</sub>	Martensite finish
M <sub>d</sub>	Martensite stabilization
A <sub>s</sub>	Austenite start
A <sub>f</sub>	Austenite finish
B2	Austenite phase
B19'	Martensite phase
R	R-phase
$\Delta H$	Changes of enthalpy energy
$\Delta S$	Changes of entropy energy
$\sigma_f$	Forward transformation stress
$\sigma_r$	Reverse transformation stress
$\Delta\sigma_f$	Forward transformation stress interval
$\Delta\sigma_r$	Reverse transformation stress interval

# **PENCERUNAN BERFUNGSI ALOI INGATAN BENTUK NiTi OLEH PENUAAN DAN PENYEPUHLINDAPAN SEPARA**

## **ABSTRAK**

Tingkah laku bentuk bentuk aloi NiTi menyampaikan daya tetap apabila beban digunakan di atasnya. Oleh itu, had untuk sebarang keadaan progresif atau perantaraan kawalan membuat aloi berfungsi hanya untuk aplikasi tindakan diskret. Untuk membolehkan kawalan yang lebih baik dalam aplikasi penggambaran, NiTi yang berfungsi secara berperingkat dicipta dengan memperkenalkan rawatan haba kecerunan di sepanjang aloi. Penyelidikan yang sebelum ini menunjukkan bahawa kecerunan rawatan penyepuhlindapan dan hamper equatomik aloi NiTi menghasilkan kemerosotan lereng dataran curam manakala rawatan kecerunan dalam aloi Ni-kaya menghasilkan ketengangan pemulihan yang baik pada transformasi terbalik. Kajian ini menerokai kesan penyepuhlindapan separa dan penuaan secara serentak menggunakan Ti-50.9at% Ni wayar yang digulung ke arah tingkah laku transformasi fasa martensit dan untuk mewujudkan wayar NiTi yang berfungsi secara berperingkat dengan meletakkan rawatan haba kecerunan sepanjang wayar. Spesimen dipanaskan pada julat suhu 300 °C hingga 550 °C selama tempoh 10, 20, 30 dan 60 minit dalam argon. Tingkah laku transformasi fasa martensit termal dicirikan dengan menggunakan imbasan calorimeter berbeza dan tingkah laku ubah bentuk memori telah dikaji dengan menggunakan mesin tegangan sejagat.

Eksperimen ini adalah untuk meneroka konsep baru NiTi yang dinilai secara berfungsi. Profil suhu kecerunan dibuat secara tempatan oleh laser CO<sub>2</sub> sepanjang wayar. Julat suhu yang berkesan untuk profil kecerunan untuk Ti-50.9at% Ni telah ditentukan pada 400 °C - 525 °C pada tempoh yang berbeza. Dua spesimen wayar diuji

dengan tempoh yang sama dan tempoh yang berlainan. Telah didapati bahawa spesimen dengan tempoh yang berbeza dalam wayar tunggal menghasilkan selang tekanan yang lebih tinggi. Satu spesimen dipanaskan secara tempatan pada suhu yang berbeza dan tempoh yang berbeza. Suhunya adalah 400 °C selama 10 minit, 475 °C selama 30 minit dan 525 °C selama 20 minit. Semasa ditarik bentuknya, wayar yang dipanaskan secara lokal dengan tempoh yang berlainan memperlihatkan selang tekanan ke hadapan yang lebih tinggi iaitu 301 MPa dan selang tekanan terbalik sebanyak 265 MPa. Perubahan yang dihasilkan sekitar 10% dan sisa ketegangan adalah 1%. Kaedah rawatan haba ini menghasilkan hasil positif dalam mewujudkan pelbagai tekanan dataran untuk kecerunan aloi NiTi berfungsi.

# FUNCTIONALLY GRADED NiTi SHAPE MEMORY ALLOYS BY AGEING AND PARTIAL ANNEALING

## ABSTRACT

A shape memory behavior of NiTi alloy delivers constant forces when load is applied on it. Thus, the limitation for any progressive or intermediate state of control makes the alloy to function only for discrete action application. To enable a better control in actuation applications, a functionally graded NiTi is created by introducing a gradient heat treatment along the alloy. Recently, few works have been reported on gradient annealing treatment of cold-worked near-equiatomic NiTi alloy to produce steeper stress plateau slope while gradient ageing treatment in Ni-rich alloy produces good recovery strain on the reverse transformation. This study explored the effect of partial annealing and ageing treatment of a cold-worked Ti-50.9at%Ni wire towards martensite phase transformation behavior and to create multiple steps of stress plateau NiTi wire by localizing the heat treatment along the wire. Specimen used in this study was a Ti-50.9at%Ni wire with a diameter of 2 mm. The specimens were heated at temperature range of 300°C to 550°C for duration of 10, 20, 30 and 60 minutes in argon atmosphere. The thermal martensite phase transformation behavior was characterized by using a differential scanning calorimeter (DSC) and the shape memory deformation behavior was studied by using a universal testing machine (UTM).

The experimental work explored a concept of functionally graded NiTi materials. The gradient temperature profile was locally created by CO<sub>2</sub> laser along its length. The effective temperature range for gradient profile for functionally graded cold-worked Ti-50.9at%Ni was determined at 400°C - 525°C at different duration.

Two specimens of wire were tested with same temperature and different duration. It was found that the specimen with different duration in a single wire produced higher stress interval. The temperatures are 400°C for 10 min, 475°C for 30 minutes and 525°C for 20 minutes. During tension, the localized heat treated with different duration exhibited forward stress interval which is 301 MPa and reverse stress interval of 265 MPa. The deformation yielding around 10% transformation strain and the residual strain is 1%. The localized laser heat treatment method executes a positive result in creating multiple steps of stress plateau of functionally graded behavior of NiTi alloy.

# CHAPTER ONE

## INTRODUCTION

### 1.1 Research Background

Shape memory alloy (SMA) is a unique material in metallic alloys group. The alloy has the capability of memorizing its original shape after being deformed beyond elastic limit. This shape recovery can be achieved instantly upon the release of the load or heated to above its critical temperature. During tension, this alloy experiences huge strain and can return to its original length upon unloading due to its ability to undergo reversible thermoelastic martensite phase transformation where the phase changes between austenite and martensite that can be induced by temperature or stress input (Otsuka & Ren, 2005). Austenite phase is stable at high temperature also known as the parent phase and the martensite phase that is stable at low temperature (Ozbulut, Hurlebaus, & Desroches, 2011). In some SMAs, this transformation can also be stimulated by magnetic (Mohd Jani, Leary, Subic, & Gibson, 2014) and electrical (Cui, Song, & Li, 2010). This transformation phenomenon can be classified as shape memory effect and pseudoelasticity. Shape memory effect refers to recovery of a deformed alloy to its original shape and size when heated to beyond its transformation temperature. Pseudoelasticity refers to the instantaneous recovery of the deformed alloy upon the release of load (Elibol & Wagner, 2015).

Figure 1.1 shows the phenomenon of the shape memory behavior of SMA in real life. Initially, the alloy rod is in straight condition. When the rod is bend at below its martensite start temperature (martensite phase), the rod remains in deformed condition upon the removal of the load, demonstrating that the deformation is non-elastic, (refer (a)). When the bent rod is heated up to above its reverse transformation

temperature (austenite phase), it returns to its original shape instantaneously. This behavior is known as the shape memory effect. At the same situation, if the rod is deformed at high temperature which is above the transformation temperature for shape recovery, the rod will recover to its original position spontaneously upon unloading, as shown in (b). This is known as pseudoelasticity.

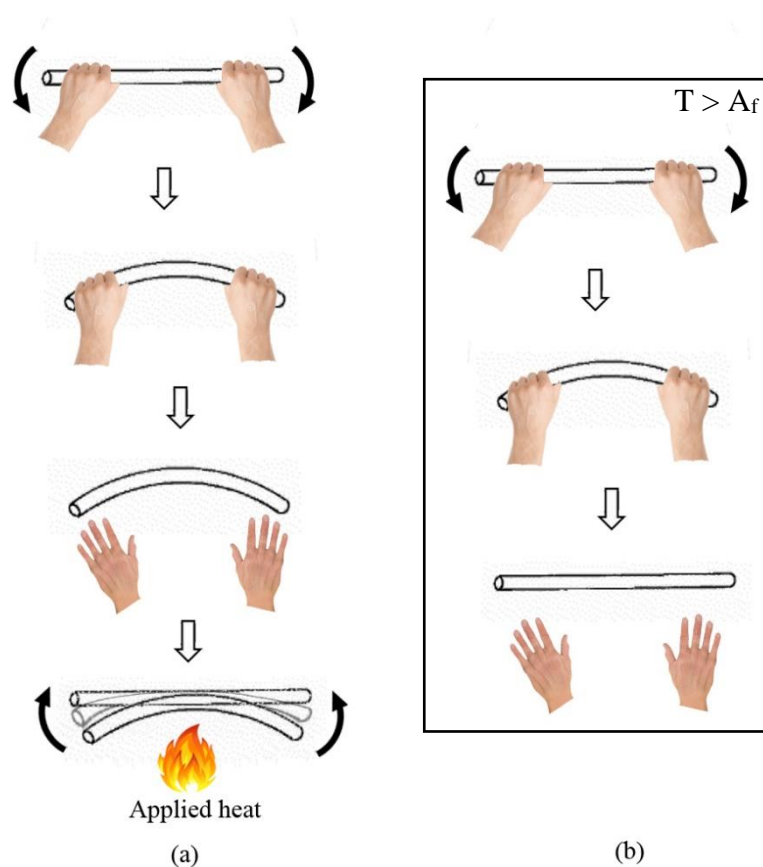


Figure 1.1. A graphic illustration of (a) shape memory effect and (b) pseudoelasticity exhibited by shape memory alloys.

There are few numbers of alloys that exhibit shape memory behavior, such as the binary Ni-Ti, Au-Cd, Cu-Zn and others, the tertiary iron-based and copper-based which are Cu-Zn-Al, Fe-Mn-Si and Cu-Al-Ni. Among all, NiTi is the most widely used for its superior shape memory behavior and much more significantly best for most applications. This is because others are impracticability and poor thermos-mechanic

performance compared to NiTi-based SMAs (Ezaz, Wang, Sehitoglu, & Maier, 2013; Lobo, Almeida, & Guerreiro, 2015).

Tensile deformation behavior of a shape memory alloy is illustrated in Figure 1.2. Thermoelastic martensitic transformation is also a mechanical deformation process. Therefore, it is possible to induce the transformation by the application of load, as is by the variation of temperature. During tensile, initially the alloy at austenite phase exhibits the linear elastic, stress plateau and hysteresis on the recovery. The upper level stress plateau resembles the forward phase transformation from austenite to stress-induced martensite, while the low level stress plateau indicates the subsequent reverse phase transformation (Seo, Kim, & Hu, 2015).

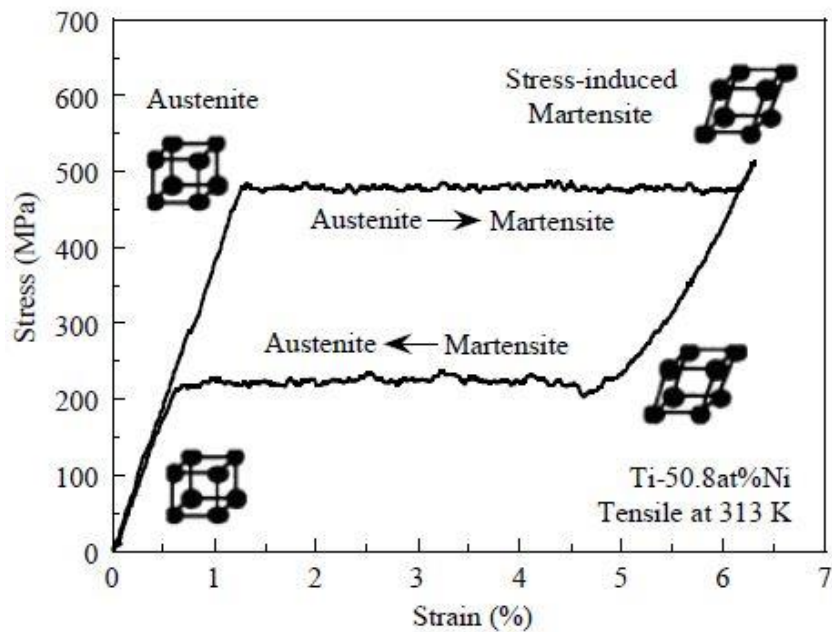


Figure 1.2. Stress-strain curve showing the pseudoelastic deformation behavior.

SMAs have the ability to recover from large deformation well beyond the normal elastic strain limits of metals. This behavior provides the material the ability to produce a mechanical work output without complex mechanical designs. Owing to the

special feature, shape memory alloys have been used widely around the world in various engineering applications and technical applications due to its unique characteristics such as orthodontic wire (Fernandes et al., 2011), actuators (Guo et al., 2015; Leary et al., 2013; Mohd Jani et al., 2014), sensors (Nespoli et al., 2010), aerospace (Barbarino et al., 2014), and biomedical applications (Morgan, 2004; Petrini & Migliavacca, 2011).

Although SMAs are widely used in many applications nowadays. A SMA can be used as or in actuators or sensors, based on the principle work output that responses to an external stimulation (Choudhary & Kaur, 2016). SMA actuators are triggered by application either stress or temperature, thus the window size of the control parameter is an important design parameter for SMA actuator applications. However, the alloys exhibit small temperature changes between the transformation phases where the bulk of the phase transition occurs within a narrow range of  $\sim 5^{\circ}\text{C}$  (Miller & Lagoudas, 2001). The stress interval of a stress-induced martensite transformation is fundamentally determined by the temperature changes interval between the start and finish transformation temperatures. Due to the small transformation temperature interval, this transformation occurs with a similar stress value that leading to zero transformation stress interval (Mahmud, Liu, & Nam, 2007). In stress-strain curve, this phenomenon is identified by a flat stress plateau over a large deformation strain of 5-8% which explains the instantaneous change of alloy over the single threshold value of stress and temperature (Shariat, Liu, & Rio, 2014). The sudden responds during deformation and recovery limits the applicability of shape memory application, especially for a case which requires intermediate or continuous control of the output. Industries found difficulties in controlling the motion of the shape memory apparatus as it requires a precise control in external input signals, either temperature or stress.

To solve this issue, it is necessary to expand the stress interval needed for stress-induced martensitic transformation along the length of the alloy to meet with the application requirement. There are three major ways that have been reported in literature to create functionally graded for the SMA such as microstructurally graded, compositionally graded and geometrically graded (Shariat, Meng, Mahmud, et al., 2017; Shariat, Meng, & Mahmud, 2017). Functionally graded and stepped alloy will be explored in this thesis by local heat treatment along an alloy wire. It would be a great advantage if step series of gradient microstructure properties can be programmed along the shape memory alloy.

## **1.2 Problem Statement**

Modifying the stress-induced martensite transformation stress plateau was possible via partial anneal treatment and ageing (Mahmud et al., 2007; Razali & Mahmud, 2015). Figure 1.3 illustrates the stress-strain curve of deformation behavior of gradient annealed of Ti-50.5at%Ni alloy. The gradient behavior yielded a good gradient of 4.7 GPa stress slope on the forward martensite phase transformation and 8.6 GPa stress slope on the reverse. The stresses and strains were calculated based on engineering strain. The stress interval achieved by the functionally graded NiTi alloy for forward stress-induced martensite transformation was 280MPa, while for the reverse transformation was 300MPa. However, the recovery of strain on the reverse transformation was not fully achieved.